PEDOT:PSS Schottky contacts on annealed ZnO films

2011 Chinese Phys. B 20 047301

(http://iopscience.iop.org/1674-1056/20/4/047301)

Chin. Phys. B Vol. 20, No. 4 (2011) 047301

PEDOT:PSS Schottky contacts on annealed ZnO films*

Zhu Ya-Bin(朱亚彬)[a)†], Hu Wei(胡 伟)[a)], Na Jie(纳 杰)[a)], He Fan(何 帆)[a)], Zhou Yue-Liang(周岳亮)[b)], and Chen Cong(陈 聪)[b)]

[a)] *School of Science, Beijing Jiaotong University, Beijing* 100044*, China*

[b)] *Beijing National Laboratory for Condensed Matter Physics, Institute of Physics, Chinese Academy of Sciences, Beijing* 100190*, China*

(Received 12 October 2010; revised manuscript received 7 December 2010)

Polycrystalline ZnO and ITO films on SiO_2 substrates are prepared by radio frequency (RF) reactive magnetron sputtering. Schottky contacts are fabricated on ZnO films by spin coating with a high conducting polymer, poly(3, 4-ethylenedioxythiophene): poly(styrenesulfonate) (PEDOT:PSS) as the metal electrodes. The current–voltage measurements for samples on unannealed ZnO films exhibit rectifying behaviours with a barrier height of 0.72 eV ($n = 1.93$). The current for the sample is improved by two orders of magnitude at 1 V after annealing ZnO film at 850 °C, whose barrier height is 0.75 eV with an ideality factor of 1.12. X-ray diffraction, atomic force microscopy and scanning electron microscopy are used to study the properties of the PEDOT:PSS/ZnO/ITO/SiO_2. The results are useful for applications such as metal–semiconductor field-effect transistors and UV photodetectors.

Keywords: Schottky contacts, rectifying characteristic, annealed ZnO film

PACS: 73.40.Sx, 73.61.Ga, 73.50.–h **DOI:** 10.1088/1674-1056/20/4/047301

1. Introduction

Schottky diodes have attracted much attention in the development of various electronic devices due to their high power and high frequency applications. Schottky contacts on conventional semiconductor silicon have been used in industry.[1] Moreover, the relevant technologies of Schottky diodes for the new generation of semiconductor GaN have been adequately investigated.[2–4] In recent years, ZnO bulk and films have attracted intensive interest for their potential photoelectric applications.[5–7] Properties such as a direct band gap of 3.37 eV at room temperature and an exciton binding energy of 60 meV are more suitable for exploiting UV light-emitting diodes,[8] UV photodetector[9] and UV random lasers.[10]

The first Schottky contacts to ZnO were reported by Mead in 1965.[11] Since then much effort has been made to explore the performances of ZnO-based Schottky contacts using Au, Ag, Pt, Pd etc. as metal electrodes. Although the barrier heights of 0.6 eV–0.8 eV were reported in the literature,[12] a number of well-known problems in the formation of Schottky contacts are still not solved. Among them, the surface states between the metal and the semiconductor, the diffusion of the metal into the semiconductor, and the contaminants can result in a low barrier height and a large leakage current. To avoid these problems, Nakano *et al.*[13] and Gunji *et al.*[14] proposed using a conducting poly(3, 4-ethylenedioxythiophene): poly(styrenesulfonate) (PEDOT:PSS) for the Schottky contact electrodes to ZnO single crystalline bulk. PEDOT:PSS is a promising Shottky contact candidate because of the following merits: work function of the PEDOT:PSS is 5.0 eV; electrical conductivity is about 300 S/cm; it is able to avoid surface damage because of the moderate fabrication processes at room temperature. Here, we report PEDOT:PSS Schottky contacts on polycrystalline ZnO films and attempt to demonstrate that the condition of the semiconductor surface will not critically affect Schottky barriers using PEDOT:PSS as metal electrodes. The quality of the ZnO thin films, such as electron density and mobility, are more important for PEDOT:PSS Schottky contacts on ZnO films.

2. Experiment

A ceramic ITO target was first located in an RF reactive magnetron sputtering chamber. High-purity argon gas (99.9999%) was ionized and bombarded the target for 40 min or so. ∼ 100 nm ITO was de-

*Project supported by the Fundamental Research Funds for the Central Universities of China (Grant No. 2009JBM098).

†Corresponding author. E-mail: ybzhu@bjtu.edu.cn

posited directly on quartz substrates at 350 °C. Then, ~ 140 nm ZnO thin films were grown on ITO/SiO_2 with Zn metal (99.9% purity) target in Argon gas and oxygen gas (99.9999%) ambient atmosphere with a partial pressure of ratio of 20:10. The growth pressure was fixed at 1 Pa and the distance between target and substrate was fixed at 60 mm. Using the spin coating method, the PEDOT:PSS films were fabricated on ZnO films, which were as-received and annealed at 850 °C in a Muffle furnace in air, respectively. A gold protective layer was evaporated on an annealed ZnO/ITO/SiO_2 structure using electron beam evaporation. The samples with an Au protective layer are labelled structure (i) and those without an Au protective layer are labelled structure (ii).

The crystal structure of ZnO/ITO/SiO_2 sample was analysed by x-ray diffraction (M18AHF, Mac Science). The surface morphology images of the ZnO films before and after annealing were investigated using atomic force microscopy (AFM) (Pico Scan(TM) 2500, MI). Scanning electron microscopy (SEM) (Hitachi S-4800) was used to observe the surface morphology images of the annealed ZnO film before and after spin coating PEDOT:PSS. Current–voltage measurement for all of the samples were performed with Keithley 2410 I-V measurement equipment.

3. Result and discussion

Typical θ–2θ scan of teh XRD patterns for ZnO/ITO/SiO_2 is presented in Fig. 1. For samples before annealing, a broad small ZnO (002) peak appears in Fig. 1, which indicates that most of the grains in the film have a c-axis orientation. In addition, ITO (222) and (411) peaks are can be clearly observed, which means that ITO is polycrystalline. The ZnO (002) peak becomes strong and sharp compared with those of the samples after annealing. Two small ZnO (100) and ZnO (101) peaks appear, as shown in Fig. 2(b). This result demonstrates that the annealed ZnO film prefers c-axis orientation with a small number of other orientation re-crystallization grains at a high temperature (850 °C).

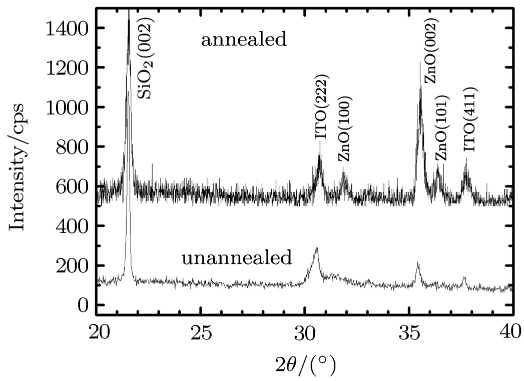

Fig. 1. The XRD patterns for the ZnO/ITO/SiO_2 multilayers.

Figure 2 shows the atomic force microscope (AFM) images of ZnO films before and after annealing. The sizes of the grains in the ZnO film before annealing are much smaller than those in samples after annealing. This result is consistent with the reported result that the grain size increases with annealing temperature increasing.[15] Hexagonal grains are clearly observed in Fig. 2(b). The root mean square (RMS) value of roughness is 19.04 nm for the sample before annealing and 27.16 nm for the sample after annealing. The fact that the RMS value increases with annealing temperature increasing is in accordance with the result reported by R. Khanna *et al.*[16]

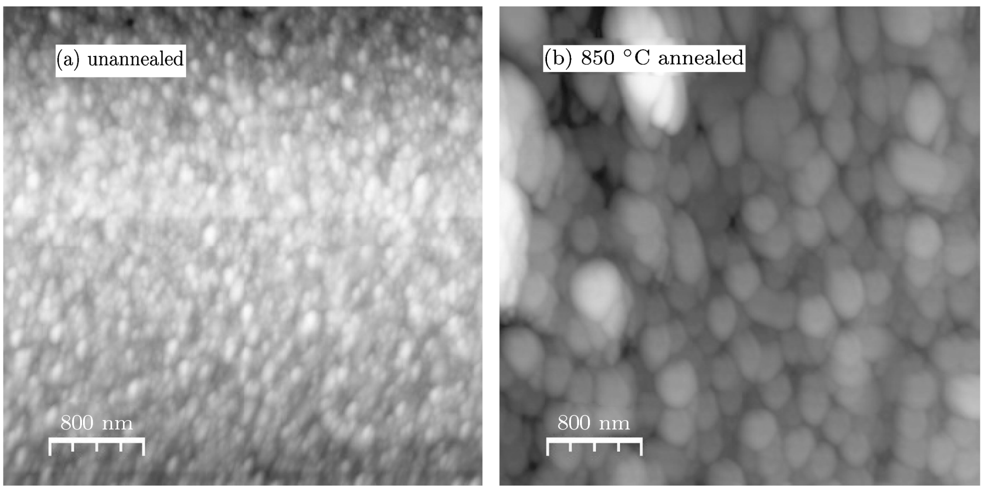

Fig. 2. AFM images for the surface of (a) unannealed and (b) annealed ZnO/ITO/SiO_2.

Figure 3 shows the surface morphology images for the annealed ZnO and PEDOT:PSS/ZnO films. The ZnO film is a flat plane with a uniform distribution of pores, as exhibited in Fig. 3(a). Figure 3(b) shows smooth continuous appearance with plenty of clusters in PEDOT:PSS/ZnO film surface. These results indicate that PEDOT:PSS covers the whole ZnO film and both are tightly combined together.

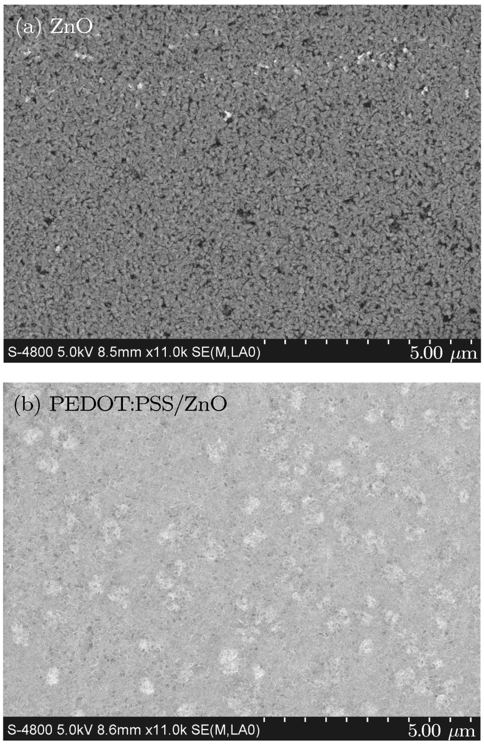

Fig. 3. The SEM images for the surface of (a) annealed ZnO and (b) PEDOT:PSS/ZnO films.

Figure 4 shows the voltage dependences of the current for samples before and after annealing. In Fig. 4(a), the current rectification ratios at ±1.5 V are of the same order of magnitude. In Fig. 4(b), the current rectification ratio improves by two orders of magnitude at ±1.5 V. The rectifying behaviour of the annealed sample is more typical than that of the unannealed sample. The turn-on voltage of the annealed sample is about 0.7 V. The results can be compared with those reported by Liu *et al.* for Au/Ni/Al-GaN diodes.[3]

Figure 4(b) shows the *I*–*V* curves with two structures. One is Au/PEDOT:PSS/ZnO/ITO/SiO_2, which belongs to structure (i) and is shown in top-left inset in Fig. 4(a); the other is PEDOT:PSS/ZnO/ITO/SiO_2, which belongs to structure (ii) and is displayed in top-left inset of Fig. 4(b). A higher current can be observed for the sample with an Au protective layer. The reason may be ascribed to much more free electrons flowing from Au to PEDOT:PSS/ZnO under the action of forward bias (positive voltage).

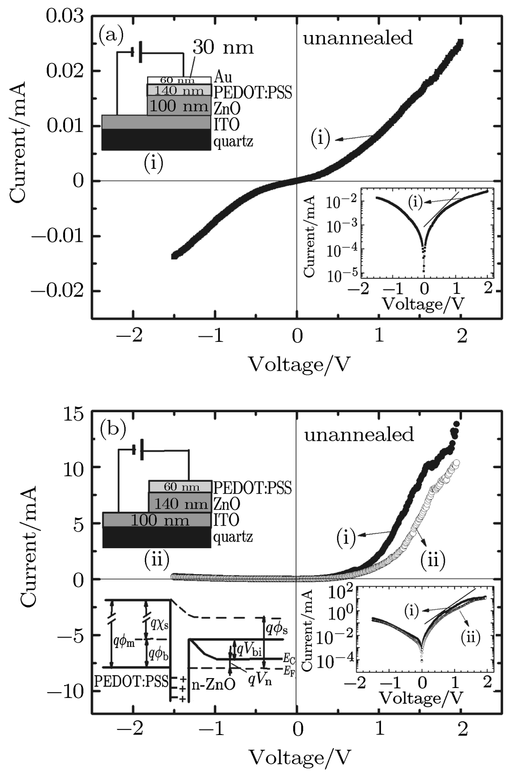

Fig. 4. Current–voltage characteristics for samples (a) unannealed ZnO film with structure (i) and (b) annealed ZnO films with structure (i) (solid circle) and structure (ii) (open circle). Structure (i) and structure (ii) are shown in top-left insets in Fig. 4(a) and Fig. 4(b), respectively. The *I*–*V* curves in logarithmic coordinate is displayed in bottom-right insets in Fig. 4(a) and Fig. 4(b), respectively. The schematic energy band for PEDOT:PSS/ZnO at thermal equilibrium state is exhibited in bottom-left insets in Fig. 4(b).

The schematic thermal equilibrium state energy band is shown in bottom-left inset in Fig. 4(b). Herein, the height of potential barrier at Schottky contact on n-type ZnO is given by

$$\phi_{\rm b} = \phi_{\rm m} - \chi, \tag{1}$$

where $\phi_{\rm m}$ is the metal work function and χ is the electron affinity of semiconductor. From the thermionic emission model, Schottky junction under forward bias has the *I*–*V* relation of

$$I = I_{\rm S} \exp\left(\frac{qV - IR_{\rm S}}{nkT}\right), \quad V \gg 3kT/q, \tag{2}$$

where $I_{\rm S}$ is the saturation current density, q is the elementary charge, V is the applied voltage, n is the ideality factor, k is Boltzmann's constant, and T is the absolute temperature. $I_{\rm S}$ is expressed as

$$I_{\rm S} = A^* S T^2 \exp\left(-\frac{\phi_{\rm b}}{kT}\right), \tag{3}$$

where A^* is the effective Richardson constant with $A^* = 36\ A\cdot cm^{-2}\cdot K^{-2}$ for ZnO[17] and ϕ_b is the Schottky barrier height. In the bottom-right inset of Fig. 4, the slope and the I intercept from the linear fit to the semilog plot for $V = 0.03\ V - 0.06\ V$ are obtained to be $n_{\text{un-anneal}}$=1.93, $n_{\text{anneal}} = 1.12$, and $\phi_{\text{b un-anneal}} = 0.72$ eV, $\phi_{\text{b anneal}} = 0.75$ eV, respectively. The Schottky barriers are lower than that reported by Nakano *et al.*,[13] probably because of the following reasons: one is that the ZnO films are polycrystalline not on high-quality single ZnO bulk; the other is that Schottky contacts with layer-by-layer have no typical ring-shaped mesa structure. However, this work indicates that with PEDOT:PSS used as metal electrodes, the condition of semiconductor surface will be less important than the quality of ZnO films. High electron density and mobility will result in high-quality PEDOT:PSS Schottky contact on ZnO films.

4. Conclusions

We have successfully fabricated PEDOT:PSS Schottky contacts on ZnO polycrystalline films. ITO and ZnO films are sequentially deposited on SiO_2 substrates by RF magnetron sputtering. Then, PEDOT:PSS is spread by a spin coating process on ZnO films before and after annealing. The Schottky contacts on annealed ZnO films show more typical rectifying behaviour. The current of Schottky contact with the Au protective layer is higher than that without Au protective layer. The best Shottky barrier is 0.75 eV with an ideality factor of 1.12. The results demonstrate PEDOT:PSS for the Schottky contact not only on ZnO single crystals but also on polycrystalline ZnO thin films.

Acknowledgement

We thank Zhang X Q and Sun J for fruitful discussion, Liu C X of Institute of Microstructure and Property of Advanced Materials, Beijing University of Technology for atomic force microscopy (AFM) measurement, and Zhang L of Institute of Chemistry, Chinese Academy of Sciences for scanning electron microscopy (SEM) measurement.

References

[1] Miura N, Nanjo T, Suita M, Oishi T, Abe Y, Ozeki T, Ishikawa H, Egawa T and Jimbo T 2004 *Solid-State Electronics* **48** 689

[2] Liu F, Wang T, Shen B, Huang S, Lin F, Ma N, Xu F J, Wang P and Yao J Q 2009 *Chin. Phys.* B **18** 1618

[3] Liu F, Wang T, Shen B, Huang S, Lin F, Ma N, Xu F J, Wang P and Yao J Q 2009 *Chin. Phys.* B **18** 1614

[4] Wang C, Feng Q, Hao Y and Wan H 2006 *Acta Phys. Sin.* **55** 6085 (in Chinese)

[5] Zhao S Q, Yang L M, Liu W W, Zhao K, Zhou Y L and Zhou Q L 2010 *Chin. Phys.* B **19** 087204

[6] Tsukazaki A, Ohtomo A, Onuma T, Ohtani M, Makino T, Sumiya M, Ohtani K, Chichibu S F, Fuke S, Segawa Y, Ohno H, Koinuma H and Kawasaki M 2005 *Nat. Mater.* **4** 42

[7] Chong M K, Abiyasa A P, Pita K and Yu S F 2008 *Appl. Phys. Lett.* **93** 151105

[8] Nakahara K, Akasaka S, Yuji H, Tamura K, Fujii T, Nishimoto Y, Takamizu D, Sasaki A, Tanabe T, Takasu H, Amaike H, Onuma T, Chichibu S F, Tsukazaki A, Ohtomo A and Kawasaki M 2010 *Appl. Phys. Lett.* **97** 013501

[9] Nakano M, Makino T, Tsukazaki A, Ueno K, Ohtomo A, Fukumura T, Yuji H, Akasaka S, Tamura K, Nakahara K, Tanabe T, Kamisawa A and Kawasaki M 2008 *Appl. Phys. Lett.* **93** 123309

[10] Cao H, Zhao Y G, Ong H C, Ho S T, Dai J Y, Wu J Y and Chang R P H 1998 *Appl. Phys. Lett.* **73** 3656

[11] Mead C A 1965 *Phys. Lett.* **18** 218

[12] Polyakov A Y, Smirnov N B, Kozhukhova E A, Vdovin V I, Ip K, Heo Y W, Norton D P and Pearton S J 2003 *Appl. Phys. Lett.* **83** 1575

[13] Nakano M, Tsukazaki A, Gunji R Y, Ueno K, Ohtomo A, Fukumura T and Kawasaki M 2007 *Appl. Phys. Lett.* **91** 142113

[14] Gunji R Y, Nakano M, Tsukazaki A, Ohtomo A, Fukumura T and Kawasaki M 2008 *Appl. Phys. Lett.* **93** 012104

[15] Özgür Ü, Teke A, Liu C, Cho S J, Morkoc H and Everitt H O 2004 *Appl. Phys. Lett.* **84** 3223

[16] Khanna Rohit, Ip K, Heo Y W, Norton D P and Pearton S J 2004 *Appl. Phys. Lett.* **85** 3468

[17] Jones F E, Wood B P, Myers J A, Hafer C D and Lonergan M C 1999 *J. Appl. Phys.* **86** 6431